Author Manuscript

Hierarchically Reconfigurable Soft Robots with Reprogrammable Multimodal Actuation

Fuyi Fang, Wenbo Li, Xinyu Guo, Huyue Chen, Guang Meng, Wenming Zhang**

F. Fang, X. Guo, G. Meng, W. Zhang

School of Mechanical Engineering and State Key Laboratory of Mechanical Systems and Vibration

Shanghai Jiao Tong University

Shanghai 200240, China

E-mail: wenmingz@sjtu.edu.cn

W. Li

School of Aerospace Engineering and Applied Mechanics

Tongji University

Shanghai 200092, China

E-mail: wenboli@tongji.edu.cn

H. Chen

University of Michigan-Shanghai Jiao Tong University Joint Institute

Shanghai Jiao Tong University

Shanghai 200240, China

This is the author manuscript accepted for publication and has undergone full peer review but has not been through the copyediting, typesetting, pagination and proofreading process, which may lead to differences between this version and the Version of Record. Please cite this article as doi: 10.1002/adfm.202414279.

This article is protected by copyright. All rights reserved.

Author Manuscript

Keywords: hierarchical reconfigurability, elastically-guided multimodal actuation, reprogrammability, soft robots.

Abstract

Reconfigurable soft robots exhibit superior flexibility and adaptability when coping with complex environments and variable tasks. However, conventional modular design strategy based on soft actuator modules with specific structure and actuation mode as the basic constructing element for reconfigurable soft robots always has limited reprogrammability or scalability. Here, we report a hierarchical reconfigurable strategy that not only offers conventional module reconfiguration as the first level to build different robot prototypes, but also provides the elastically-guided multimodal actuation (contraction, bend and twist) as the second level which can be reprogrammed to construct different actuator modules. This strategy deepens the modularity to a higher dimensionality and provides more choices for robots to adjust various conformations and functions as needed, for example, a peristalsis robot, an omnidirectional crawling robot and a soft manipulator can be easily constructed using the module level reconfiguration. Moreover, soft manipulators with various preprogrammed deformation trajectories based on the mode reconfiguration are proved to dramatically reduce the operation difficulty and cost in potential applications such as environment detection and human-robot interaction. This work provides a hierarchical framework for reconfigurable soft robots and may open up a new way for modular design.

1. Introduction

Reconfiguration is a way of deconstructing and reassembling complex systems to realize multiple functions, providing them with unprecedented flexibility and versatility[1]. Recent years have seen the introduction of reconfiguration strategies in the field of soft robotics[2], and these strategies have been the driving force behind a new wave of soft robots. Like building blocks, reconfigurable soft robots

This article is protected by copyright. All rights reserved.

Author Manuscript

comprise various kinds of functional elements that can be easily disassembled and remounted into any desired forms. While the specificity is that reconfigurable soft robots have flexible external features and are driven by soft actuators[3]. Multiple types of soft actuators have been applied to reconfigurable robots, such as pneumatic actuators[4], magnetic actuators[5], dielectric elastomer actuators[6], gel actuators[7] and other actuators composed of smart materials[8], which inherit the safety and pliability of flexible bodies, thus enabling tasks that traditional rigid robots are limited, like grasping fragile objects[9] and adapting to unstructured environments[10]; on the other hand, the reconfiguration strategy revolutionarily provides soft robots with the advantages of reusability, interchangeability and scalability, which allows the soft robots to be easily adjusted to the structures as needed, reducing the redesigning time and further the manufacturing cost, and improving the versatility of products[11].

There have been a series of researches for reconfigurable soft robots. One method is based on the modularization strategy[11a, 12], i.e., by designing a set of modules with different actuation modes and combining them to obtain the desired motions. These modules usually have a single actuating mode, such as contraction[4c, 13], elongation[14], bend[15], and twist[16], while several sophisticatedly designed modules are able to realize multiple modes or coupling of several modes[17], for instance, some delicate origami-based actuators have achieved the integration of all functions on one unit, which significantly improve the feasibility of soft modules[18]. Some smart gels also perform remarkable multi-mode actuation according to different stimuli or programmed instructions, like the temperature responsive gels[19], photon responsive gels[20] and the DNA programed gels[21]. These actuators are important precursors to modular soft robots. To easily recombine, modules are designed with common and reversible connection methods, such as plug-and-play[18, 22], mortise-and-tenon[17a, 23], buckles[24], etc., allowing series connection, parallel connection or any other arbitrary connection patterns. Modular actuators are widely applied on series connected robotic arms which require complex and composite manipulation[25], at the same time, this way promises the functions of the robotic arms to be changeable owing to the inherent reconfigurability which is concomitant with modularity. Although the modularization strategy offers the robots the advantages of mass manufacturing, easy maintenance, and raises the utilization rate of the components, there is still room for improvement in terms of convenience. For example, if the assembled robot needs to adjust the function, or a local damage occurs, it has to replace the entire module, thus separate the pre and post

This article is protected by copyright. All rights reserved.

Author Manuscript

ones, remove the target module, and reassemble with a new one, which is burdensome and especially unfriendly for the rearrangement of power lines, signal wires or air tubes.

On the other hand, the majority of existing modules are designed with a fixed structure and function. Consequently, reconfiguration is only possible by replacing modules with different modes. The few modules that can be reconfigured through reprogramming generally require complex structural designs and multi-driver combinations corresponding to numerous control channels. This increases the complexity and difficulty of the control system. Alternatively, the complexity can be reduced by adding constraints to the frame or exoskeleton[24, 26], comparing with modularization strategy, the exoskeleton extracts the functional element that induces deformation from the modules, and further provides a generalized way to reassemble and reprogram, which significantly improves the convenience when adjusting robot modes. However, existing reconfigurable exoskeletons also show their limitation in non-scalability. They are usually of an integrated design, which means that a set of exoskeletons are only suitable for a certain robot. For instance, most soft manipulators equipped with designed exoskeletons are not allowed to change the length, because the different lengths require another set of exoskeletons. Lacking standardization and uniformity makes it difficult to achieve expansion of the robots and limits their functionality.

Creatures in nature are composed of organs, which in turn are composed of various tissues[27], and such organization makes creatures well-adapted and extremely controllable. Also, such strategy is used in new materials, like hierarchical designs in molecular level and structure level.[7a, 8d] Inspired by this hierarchy, we propose a new concept of hierarchically reconfigurable strategy to deepen the conventional reconfiguring strategy to a more profound level which can significantly improve the scalability and adaptability of soft robots. We also make a simple categorization of functional elements for the module and break it down into reconfigurable ones (elastic elements and actuator elements), as well as standardize and generalize the connection methods of each element so that they can be easily assembled and replaced. This way brings the advantage that we can deal with the process of actuation and deformation independently, which means that the modules are able to change the modes just by adjusting the elastic elements, but without replacing the actuator elements. We still retain the ability to arbitrarily combine modules with each other, making the modules scalable in both series and parallel dimensions. On this basis, we enable modules to switch between multiple actuating modes by regulating the elastic constraint with exoskeletons for the contraction deformation of

This article is protected by copyright. All rights reserved.

Author Manuscript

actuators. Through simulating and testing multiple actuating modes with different elastic beams and inputs, we reveal the elastically-guided mechanism, which is a passive deformation method with a single actuator, but not requiring multi actuators to achieve different modes. Instead of the formed exoskeletons which are specialized for certain robots, this elastic-beam based exoskeleton is generalized for all modules. This strategy avoids replacing the entire module to change the modes and for the damaged modules, they only need to be replaced precisely with the corresponding elements, which reduces the repairing cost for robots even more. According to this hierarchically reconfigurable strategy that deepen the modularity to a new level, we have demonstrated the multi-level reconfigurable applications, including tube detecting robot and planar omnidirectional crawling robot. We have also designed a variety of soft manipulators to realize functions such as crossing obstacles and delivering bouquets of flowers to show the prominent versatility.

2. Result and Discussion

2.1. Conception and methodology

2.1.1. Hierarchical reconfiguration

To advance reconfiguration to the next level, we consider the extraction of functional elements within the modules. As shown in **Figure 1**, the module consists of an actuator element, some elastic elements and end boards. Among these, the actuator element is centered between the two end boards to provide uniform driving force for the entire module. Contraction mode is chosen as the basic deformation of the actuator element, such as McKibben actuator, fiber reinforced actuator, foam actuator and other actuators capable of contracting, they can all be used as the actuator element. This work adopts a vacuum pressure origami actuator, which consists of a capsule heat-sealed with TPU membrane and an internal folded PET skeleton. By vacuuming the internal chamber of the capsule, the folded skeleton compacts and collapses under the compressive effect of the sealed case, thus drives the actuator's contraction; as the chamber connects to the atmosphere, the elastic energy stored in the skeleton is released, and holds the actuator back to its original state (See Figure S2 in the

This article is protected by copyright. All rights reserved.

Author Manuscript

Supporting Information for the fabrication process). The actuator can contract up to 55% and still maintain 50% contraction rate according to a load of 2 N, providing excellent performance for our proposed module. Furthermore, the actuator is convenient and cheap to manufacture owing to its commercial materials. The elastic elements are beams made of PET sheets that are cut into the desired shapes according to the different actuating modes, for example, straight beams guide the actuator to contraction or bend, and leaned beams guide the actuator for clockwise or counterclockwise twist. Parameters such as beam thickness, length, etc. have effects on the actuating performance, and more details are discussed in Section 2.3. The end boards are terminals that connect the actuator elements and the elastic elements, transmitting the force during the actuating process, and also serve as a bridge for interconnecting multiple modules. The end boards are designed with mortise-tenon and buckle structures for quick mounting and replacing between actuator elements, elastic elements as well as multiple modules.

2.1.2. Reprogrammable multimodal actuation

The actuating process of the module can be divided into two stages, i) After applying vacuum pressure to the origami actuator, the end boards are pulled together and transmit the force to the elastic beams, which are further collapsed under pressure due to the presence of outward pre-bending, resulting in simultaneous axial compression and circumferential expansion of the module, just similar to biological muscles; ii) As the vacuum is withdrawn, the elastic beams quickly release the potential energy and the module returns to its original state. The contract force of the origami actuator and the restore force of the elastic beams are shown in Equations (1) and (2).

$$F_{actuator} = F(\theta, \Delta p) - K(L_0 - Dsin\theta) \tag{1}$$

$$F_{beam} = C\left(\int_0^{\frac{\pi}{2}} \frac{d\varphi}{\sqrt{1 - sin^2\frac{\partial}{2}sin^2\varphi}}\right)^2 \tag{2}$$

In which, F in Equation (1) is the contractile force of the origami actuator about the skeleton final angle θ and the vacuum pressure. L_0 and D indicate the initial span and length of the skeleton segment. K is the elastic coefficient, which contains the shape parameters and Young's modulus of

This article is protected by copyright. All rights reserved.

Author Manuscript

the skeleton. C in Equation (2) is also a coefficient but of the elastic beams. ∂ represents the angle between the end of the beam and the end board. More details are shown in Supporting Information Text. 1 and Figure S7 to S8.

It is worth mentioning that different beams induce multiple actuation modes, for example, three elastic beams symmetrically distributed in the circumferential direction induce contraction mode; after removing an elastic beam, due to the uneven distribution of supporting force, the module will bend in the direction of no supporting force, i.e., the direction where the elastic beam is absent; if the three straight beams are replaced by leaned beams, the end boards give the elastic beams circumferential torsion in addition to the force of axial compression of the elastic beams, due to the fact that the combined force on the beams is deflected in the axial direction, as shown in Figure S11 of the Supporting Information, causing the entire module to twist; similarly, by reversing the elastic beams into chirality, the module will twist in the opposite direction.

2.2. Reconfiguration Strategy

In order to achieve modularity and reconfigurability, we have designed fast connection methods between and within modules. As shown in **Figure 2**, the hierarchical reconfigurability can be divided into the 1st level - module reconfiguration and the 2nd level - actuating mode reconfiguration. According to the structural characteristics, the connection can be further divided into mortise-tenon connection and buckle connection. Comparing with traditional pin joints and ball bearing joints, these connection methods constrain most of the freedoms on the junctions, and require no actuator to restrict, thus reduces the difficulty of controlling, also, they are designed tiny and light, and are really convenient to assemble and disassemble, which is suitable for hierarchical reconfiguration. There is a rotational process in the mortise-tenon connection, which naturally lacks the constraint of a rotational degree of freedom, and therefore the load-bearing capacity for the longitudinal direction is much higher than that for the transverse direction, and experiments have shown that the single mortise-tenon structure can carry a longitudinal force of more than 25 N, while it is disengaged due to the rotation of the tenon structure after the application of a 10 N tension force in the transverse direction (Supporting Information Figure S12), thus mortise-tenon construction is suitable for situations where the longitudinal force is high and the transverse force is low; the buckle connection has an outstanding

This article is protected by copyright. All rights reserved.

Author Manuscript

bearing capacity in both the longitudinal and transverse directions, and is suitable for the case where the force is applied in multiple directions. Experiments show that the snap structure used in this work can carry more than 20 N of force in both the longitudinal and transverse directions. As shown in Figure 2a, the series connection between modules in the 1st level reconfiguration is achieved by mortise-tenon structure, in which the tenon on the end board of the tail of one module is inserted into the mortise on the head of the other module and rotated to form a fastened connection, and the mortise-and-tenon structure ensures the axial stabilization of the modules when tensile stress is generated due to the contraction and expansion of the modules between each other. Figure 2b shows how modules are connected in parallel in the 1st level reconfiguration, i.e., the end boards of two modules are connected by a bridge, and the key on the bridge snaps into a hole at the edge of the end board; the holes symmetrically and circumferentially distribute around the edge of the end board, meaning that the modules can be easily interconnected and are of high scalability. In the 2nd level reconfiguration, the portion of the actuator that connects to the end boards is always subjected to tensile force, so we choose mortise-tenon joint, with four matching tenon elements on the actuator to serve as a medium for fixing and force transmitting. As for the mode reconfiguration, replacing the elastic beams can induce various modes of the module. The wedge-shaped clips at the two ends of the elastic beam can be elastically deformed when they are snapped into the slots on the end boards, since the elastic beam is an elastic thin sheet structure, making it easy to install and remove. Besides, as we design the width of the slots larger than the thickness of the elastic beams, the beams have some space to rotate in the slots, and we adopt a crease between the clip part and the main part of the beams, allowing the main part to rotate as the clip part is fixed on the end board. This design is about to adding a hinge between the end boards and the elastic beams, instead of just bonding them together, which leads to better performance of the modules, as is discussed in Supporting Information Text 1. Through the design of these connection structures, the modular soft robots have the capability to be quickly expandable and reprogrammable, and exhibit outstanding performances.

2.3. Characterization of Module Actuators

To further optimize the actuating performance of the modules, we have tested each mode with according properties, considering that the modules focus on different functions. Firstly, the contraction mode of module is often used in load situations, such as lifting heavy objects, muscle

This article is protected by copyright. All rights reserved.

Author Manuscript

contraction, etc. Therefore, we focus on the load capacity of the contraction module. Supporting Information Figure S14 shows the thrust generated by the compressed frame (a module without actuator), i.e., the resistance that the actuator is subjected to when it contracts. The external load that the entire module can withstand is the force of the actuator's contraction minus the resistance of the elastic beams, so that less thrust results in a greater external load capacity of the module. By increasing the length of the elastic beams from 135 mm to 165 mm, the thrust generated by the frames decreases from 0.75 N to 0.6 N. However, as the thickness of the elastic beam varies from 0.4 mm to 0.3 mm, the thrust decreases by a factor of 2.9 (0.4 mm:1.25 N, 0.3 mm:0.43 N). The thickness of the elastic beams significantly affects the frame thrust more than the length, so we use thinner elastic beams in the following tests when selecting the inducing element. Further, we incorporate the actuator into the module and test the longitudinal displacement and circumferential expansion of the contraction module under different vacuum pressure conditions, as shown in Supporting Information Figure S15. Notably, the length of the elastic beams shows a greater influence than the thickness in the circumferential expansion experiments, and the expansion rate of the module with the longest elastic beams (165 mm: 54%) is about 1.75 times larger than that of the shortest one (135 mm: 31%), while the expansion rate of the module with the thinnest elastic beams (0.3 mm: 54%) is only 1.06 times larger than that of the thickest ones (0.4 mm: 51%) under the same vacuum pressure. We choose 0.3 mm thick and 135 mm long elastic beams for simulation and experiment to verify the overall loading capacity of the module, as shown in **Figure 3**a, we hang the contraction module and drop a weight underneath to test the contraction rate of the module under different vacuum pressure. In the simulations, we simplify the action of the actuator as a tension force and apply on the center of the end boards, and the magnitude of the tension force is determined by Equation (1). Experiments and simulations show that the contraction module is still able to maintain a 30% contraction rate under a 400 g load and -80 kPa vacuum pressure.

In bend mode, the asymmetric support of the elastic beams causes a moment on the end board when the actuator contracts, leading to tilt. The supporting force of the remaining elastic beams has an effect on this rotational moment, so we simulate and test the change in the angle between the two end boards considering the thickness of the elastic beams as the dependent variable. As shown in Figure 3b, the lower end board of the bending actuator is fixed, different vacuum pressures are applied to the origami actuator, and the upper end board is tilted to form an angle with the horizon, so that

This article is protected by copyright. All rights reserved.

Author Manuscript

the bending module guided by the 0.2 mm-thick elastic beams can be bent up to the maximum of 45°when the vacuum pressure reaches -80 kPa.

The twist mode is realized by the leaned beams guidance. During the compression of the module, the leaned beams are deflected from the vertical direction by the force of the end board, which generates a torsion force in the lateral direction, and the magnitude of this force is related to the shape of the leaned beams. We define the beam shape in terms of height and leaned angle, and perform simulation and test of the twist angle as a function of the beam height H and leaned angle α, respectively. The chiral symmetry of the clockwise-twisted and counterclockwise-twisted actuator is not analytically significant, so we choose to analyze the left leaned elastic beams and the counterclockwise-twisted modules. As shown in Figure 3c, the lower end board of the module is fixed and the upper end board torsions while contracting. The twist angle increases significantly as the height of the elastic beams decreases. As for another parameter, the leaned angle of the beam affects the lateral force of the beam, and the tests show that the maximum twist angle of the module exists only when the leaned angle of the elastic beam is kept within a range, and the module has the maximum twist angle as $\theta = 40°$ when the leaned angle $\alpha = 45°$.

The performances of the different modes provide a database for the application, for example, the specific contraction rate, bend and twist angles required by the robotic arm can be found in the database for the corresponding beam parameters and vacuum pressure, which allows a guided reprogramming of the arm. In addition, some special properties of the modules also offer potential for other applications, such as the circumferential expansion in the contraction mode, which offers the possibility of fixing the module inside a narrow space.

2.4. Reconfigurable soft robots

2.4.1. A tube-climbing soft robot with 1st level reconfiguration

To verify the module reconfiguration, which is the 1st level of the hierarchical reconfigurability, we built several classic robots with the proposed modules. Firstly, we connected the contraction modules in series to mimic the motion patterns of earthworms. As shown in **Figure 4**a, earthworms

This article is protected by copyright. All rights reserved.

Author Manuscript

achieve peristalsis in subterranean passages through the expansion and contraction of the segments with the help of longitudinal muscles and circular muscles. When the longitudinal muscles excite, the segments contract longitudinally and expand transversely, and when the circular muscles excite, the deformations caused by the longitudinal muscle are restored to their original state. Our module resembles a segment of an earthworm in that the actuator plays the role of the longitudinal muscle during actuation, while the elastic beams are like the circular muscles to restore the deformation produced by the actuator. We connect three contraction modules in series and control the on-off of the vacuum source through solenoid valves, respectively, as shown in Figure 4b. One period of the earthworm robot's motion can be divided into five steps, with the same time for each step, which is defined by τ. The module Ⅰ firstly contracts, anchoring the inner wall of the tube; then the middle module Ⅱ contracts, and drags the module Ⅲ forward; as the module Ⅲ subsequently contracts, the three modules all anchor to the wall; after that, the module Ⅰ and module Ⅱ recover in turn and move forward; finally, the module Ⅲ recovers and the robot enters into the next circle, with a forward distance of 2 times of the contracted length. As shown in Figure 4c, the tethered earthworm robot equipped with a camera crawls inside a horizontal tube with $\tau = 0.2$ s for each step, and its speed is 6.7 mm/s. When crawling in a vertical tube, the earthworm robot needs to overcome the gravity of itself and the camera, so the anchoring force should be strengthened. We increase the duration of each step to $\tau = 0.5$ s to make the expansion process of the module more adequate, and accordingly, the crawling speed of the earthworm robot is sacrificed, and its upward crawling speed is 3.1 mm/s. Video S1 shows the earthworm robot crawling inside the horizontal and vertical tubes, demonstrating its potential for probing in narrow areas. We also achieve the untethered robot by integrating the control system and pump on the modules, as shown in Figure 4g and Video S2, the integrated control system is shown in Figure S18. The speed of the robot is 1.4 mm/s, which is much slower than the tethered one, owing to the lower power of the vacuum pump and the additional inertia caused by the whole control system.

2.4.2. An omnidirectional crawling soft robot with 1st level reconfiguration

After verifying the serial functionality between modules, we reconfigure the existing modules to further verify the parallel connection. As shown in **Figure 5**a, we connect three contraction modules

This article is protected by copyright. All rights reserved.

Author Manuscript

in parallel to form a triangular structure with omnidirectional movability in the plane. The movement of parallel robots relies on asymmetric actuation of modules: initially, the barycenter of the robot is at the geometric center, and when one of the actuator contracts, the barycenter is biased towards the contracted side, resulting in the front of the robot being supported by a force greater than that on the back, and therefore leading the asymmetric friction, i.e., $F_{f1} > F_{f2}$. The rapid contraction of the actuator also causes the front foot to jump forward, and when the actuator is recovered to its initial state, the front foot is anchored due to the larger friction, driving the entire robot forward. The actuated modules can be single or multiple, allowing the robot to move in 6 directions and therefore reach any positions on the plane. In order to further improve the actuation performance of the omnidirectional crawling robot, we optimize the driving frequency of the modules. The experiments are conducted using a uniform vacuum source of -50 kPa, and the robot's moving speed is tested at 0~20 Hz driving frequency under single-module and double-module actuation, respectively. Video S3 shows the motion of the tethered robot in both actuating modes. The single-module actuated robot moves the fastest as 47 mm/s with 14 Hz, while the double-module actuated robot shows a bit higher frequency than the single-module, which is 15 Hz, and the motion speed is 34 mm/s. The double-module actuation robot moves slower because of the less deviation of the barycenter. There are two reasons for this phenomenon. Firstly, the double-module actuation robot deforms less with the uniform vacuum source compared with the single one, owing to the air in the two modules has no time to escape adequately and the origami actuator could not contract to the ideal rate. Secondly, the geometric shape of the robot determines that the barycenter is farther from the pivot of the single-module than of the double-module, as seen in Figure S19, which means that the barycenter will deviate more in single-module when actuated. These two aspects lead to the difference in moving speed.

2.4.3. Reprogrammable Manipulator with 2nd level reconfiguration

Omnidirectional crawling robots of parallel connection and earthworm robots of series connection demonstrate module reconfiguration as the 1st level reconfigurability, while mode reconfiguration pushes it to the 2nd level. **Figure 6**a and Video S5 demonstrate the ability of a soft manipulator to cross an obstacle and detect objects, which is adapted to the arbitrary obstacle as a

This article is protected by copyright. All rights reserved.

Author Manuscript

tandem consisting of three bending modules and two contracting modules, with a camera mounted on the end module. The dynamic adaption of this modular robot manipulator can not only be accomplished through sequential instructions to the modules, but can also be locally adjusted using controlled vacuum pressure. Initially, the modules on the soft manipulator are all in an inactive state, located on one side of the obstacle, but the manipulator is not allowed to bend directly in this condition, or it will collide with the obstacle, so the contraction modules are firstly actuated by a high vacuum pressure of -80 kPa, which shortens the length of the manipulator by 30% as a whole, and then a vacuum pressure is applied to the bend modules at the bottom to deflect the manipulator across the obstacle; after that, the rest module on the top bends so that the camera points to the orientation of the target object, but the view is still blocked by the obstacle; as mentioned in Section 2.3, the performance of the module is also affected by the vacuum pressure, so the pressure of the contraction modules is dynamically adjusted to slowly decrease from -80 kPa to -40 kPa, and ultimately, the camera accurately points at the target object.

With the 1st level of reconfiguration already in place, the 2nd level of reconfiguration still allows for convenient adaptation of localized actuation modes. Figure 6b and Video S6 show another manipulator consisting of four modules, with the bottom module in bend mode. When the top three modules are in contraction mode, the bottom module points forward; replacing the straight elastic beam of the top modules with leaned beams, the manipulator twists to 40°, 80°, and 120° respectively with different number of replaced modules; and by flipping the leaned beams to chiral form, the manipulator then twists counterclockwise to -40°, -80°, and -120°. The 2nd level of reconfiguration empowers the manipulator to be reprogrammable and can be customized to adapt to different tasks, as shown in Figure 6c and Video S7, which also consists of five modules, we reprogram the manipulator into a bouquet deliverer that can perform tasks interacting with human.

3. Conclusion

The hierarchically reconfigurable and reprogrammable actuation strategy shows its prospects in soft robots, especially for the variable sceneries. We present the potential applications with vacuum powered modules and elastically guided exoskeletons, the demonstrations such as in-tube inspection, planar omnidirectional mobility, and more typically, the adjustable soft manipulators progressively

This article is protected by copyright. All rights reserved.

Author Manuscript

illustrate the versability of this strategy. The universal connection methods between and within the modules make multi-level reconfiguration convenient, and more importantly, the mode reconfiguration guided by replaceable elastic beams allows modular robots to avoid the replacement of the whole module, and has lower time cost in terms of adjusting the robot's function or replacing the damaged elements. On the other hand, compared with the exoskeleton based soft robots, this strategy allows the system to expand without redesigning the robot body or exoskeletons, owing to the extraction of the functional elements for the modules and independent design for the elements. Further, we establish the sequential operation system for the modular robot and the fine-tuning method for the actuation of individual modules, demonstrating that the proposed robotic system has excellent maneuverability and is more adaptable in complex situations, some more exquisite operations with changeable modes and tunable input pressure are promising in the future. The robots have shown their robustness in the experiments, and the only failure risk is the air leakage of the vacuum powered origami actuator, just like all the pneumatic actuators. However, although in the event of the actuator malfunction, the consequence is a reduction in performance of the actuator rather than a complete failure, the module can still keep working. The proposed hierarchically reconfigurable robot surpasses conventional modular robots in terms of universality, especially in fabrication, assembly, and adjustment. It also enlightens the design strategy for the traditional soft robotics, not just limited to modular soft robots, as the multi-level layout chunks the soft robot into more disaggregated sections, such as morphing elements, restriction elements, connection elements, etc., and design them respectively with higher degree of freedom, instead of the integrated but confined structures. It may provide another design philosophy for soft robots.

Despite having shown great adaptability, our showcased soft robot still lacks some specific modes such as elongation or bend-twist coupled motion. This is mainly related to the actuator element, the elongation type actuator can guide an elongation mode, while the torsion type actuator can guide a bend-twist coupled motion under the guidance of the asymmetric distributed beams. Therefore, under our proposed strategy of hierarchical reconfiguration, it is still necessary to explore more types of interchangeable actuators in expanding the actuation modes and applications of modular soft robots. On the other hand, although the origami actuators we utilized can afford loads like camera, flowers and the modules, they are still not forceful enough for some industrial applications, such as carrying a weight, lifting tools, etc. There are two ways forward in the future. Firstly, minimizing the modules to release their potential in medical fields, which require relatively lower force. It means the

This article is protected by copyright. All rights reserved.

Author Manuscript

smallest design of the actuator elements, elastic elements and end boards, and also presents a great challenge for the connection methods. Some gel, polymers or other smart materials may also be applied as the actuator, and two-photon photopolymerization is a potential technic to manufacture tiny components like end boards, beams and connectors. Secondly, it is fortunate that all of our elements are replaceable, thus a more powerful actuator element is required to substitute for the now available actuators, which can address heavy loaded situations and expands its applications further. Also, for mobile applications, equipping with a powerful actuator and beams of larger Young's modulus may help the module to leap up, and allow the modules to cope with more complex terrains.

To summary, this new concept of hierarchically reconfigurable strategy deepens the modularity to a higher dimensionality and provides more choices for soft robots to adjust various conformations and functions as needed. The reprogrammable multimodal actuation enabled by the proposed elastically-guided mechanics design for actuator module plays a key role in this hierarchical framework for reconfigurable soft robots. The combination of mode reconfiguration and module reconfiguration may open up a new way for modular design, and provide higher design freedom and scalability for the modular soft robots.

4. Methods

Origami actuator preparation: The constrictor we utilized in this work was an origami actuator, which was composed of PET skeleton and TPU skin. The manufacturing process could be summarized into 4 steps: (1) prepare two rectangular pieces of TPU membrane with size of 40×150 mm and thickness of 0.1 mm; (2) prepare a piece of PET sheet with size of 20×130 mm and thickness of 0.3 mm, fold the sheet into serrated shape, each sawtooth is 10 mm in width; (3) overlap the two TPU membrane together and seal three sides with a sealing machine *Deli group 2133*; (4) put the PET skeleton into the chamber formed by the TPU membranes as well as the gas tube, and finally seal the last side of the chamber. The whole process was operated by hand within 10 minutes.

Elastic beam preparation: The elastic beams were also fabricated with PET sheet, we chose various sizes of beams to test, especially the thickness and length of the straight beams, as well as the height

This article is protected by copyright. All rights reserved.

Author Manuscript

and angle of the leaned beams. For straight beams, we trialed thickness of 0.2 mm, 0.3 mm, 0.4 mm with the beam length of 135 mm, as well as multiple length of 120 mm, 135 mm, 150 mm with the unified thickness of 0.3 mm. For leaned beams, the thickness was 0.3 mm in standard, we tested beam height of 100 mm, 120 mm, 140 mm with the leaned angle of 45 °, as well as the leaned angle of 30 °, 45 °, 60 ° with the height of 100 mm. The clip parts of the beams were all the same, we designed the clip part as a wedge-shape and two notches to be inserted firmly in the board slots. The sizes of the beams and clip were shown in Figure S4. All the PET beams were cut by the laser cutting machine *Borui 1390*.

End boards preparation: The end boards, actuator connectors and parallel bridges were fabricated by a light-curing 3D printer *Formlabs, Form 3+* with white resin. We designed a deep slot on the bottom of the actuator connectors so that the actuator end could be inserted into the slot and glued together. Then the actuator and end boards were connected as the end boards and actuator connectors assembled by mortise-tenon structure. The tenon structure of the end boards and the actuator connectors were the same, and the key sizes of the tenon structure were marked in Figure S3. As well as the mortise structure, they were all in the same sizes on the end boards, and were also marked in Figure S3.

Control system: As for the power source and control system, we utilized a vacuum pump that could provide a vacuum pressure up to -100 kPa. In order to maintain a specific and stable pressure, we then connected a regulating valve and a digital pressure gauge to the power source. The sequence control was achieved by several groups of relay and solenoid valve, each group controlled a module or several modules of the same motion. An Arduino Nano board was connected to the relays to program the motion sequence of the modules. More details about the control system were described in the Supporting Information Text 2 and Figure S18.

Supporting Information

This article is protected by copyright. All rights reserved.

Supporting Information is available from the Wiley Online Library or from the author.

Author Manuscript

Acknowledgements

This work was supported by the National Natural Science Foundation of China (12032015, 12121002, 12002204), Research Project of State Key Laboratory of Mechanical System and Vibration (MSV202407), the Fundamental Research Funds for the Central Universities in China, the Shanghai Gaofeng Project for University Academic Program Development.

Received: ((will be filled in by the editorial staff))

Revised: ((will be filled in by the editorial staff))

Published online: ((will be filled in by the editorial staff))

References

[1] a)W. W. Lee, Y. J. Tan, H. Yao, S. Li, H. H. See, M. Hon, K. A. Ng, B. Xiong, J. S. Ho, B. C. K. Tee, *Sci. Robot.* **2019**, 4, eaax2198; b)Y. Alapan, A. C. Karacakol, S. N. Guzelhan, I. Isik, M. Sitti, *Sci. Adv.* **2020**, 6, eabc6414; c)H. Gu, M. Moeckli, C. Ehmke, M. Kim, M. Wieland, S. Moser, C. Bechinger, Q. Boehler, B. J. Nelson, *Nat. Commun.* **2023**, 14, 1263; d)J. Pei, L. Deng, S. Song, M. Zhao, Y. Zhang, S. Wu, G. Wang, Z. Zou, Z. Wu, W. He, F. Chen, N. Deng, S. Wu, Y. Wang, Y. Wu, Z. Yang, C. Ma, G. Li, W. Han, H. Li, H. Wu, R. Zhao, Y. Xie, L. Shi, *Nature* **2019**, 572, 106.

[2] a)B. Yang, A. M. Nasab, S. J. Woodman, E. Thomas, L. G. Tilton, M. Levin, R. Kramer-Bottiglio, *Adv. Mater.* **2024**; b)S. Li, R. Batra, D. Brown, H.-D. Chang, N. Ranganathan, C. Hoberman, D. Rus, H. Lipson, *Nature* **2019**, 567, 361.

[3] J. Wang, D. Gao, P. S. Lee, *Adv. Mater.* **2021**, 33, 2003088.

[4] a)T. Ching, J. Z. W. Lee, S. K. H. Win, L. S. T. Win, D. Sufiyan, C. P. X. Lim, N. Nagaraju, Y.-C. Toh, S. Foong, M. Hashimoto, *Sci. Robot.* **2024**, 9, eadk4533; b)Y. Zhai, A. De Boer, J. Yan, B. Shih, M. Faber, J. Speros, R. Gupta, M. T. Tolley, *Sci. Robot.* **2023**, 8, eadg3792; c)M. Feng, D. Yang, L. Ren, G. Wei, G. Gu, *Sci. Adv.* **2023**, 9, eadi7133; d)X. Guo, W. Li, F. Fang, H. Chen, L. Zhao, X. Fang, Z. Yi, L. Shao, G. Meng, W. Zhang, *Sci. Adv.* **2024**, 10, eadk3855.

This article is protected by copyright. All rights reserved.

Author Manuscript

[5] a)Y. Zhang, C. Pan, P. Liu, L. Peng, Z. Liu, Y. Li, Q. Wang, T. Wu, Z. Li, C. Majidi, L. Jiang, *Nat. Commun.* **2023**, 14, 4428; b)Z. Chen, Y. Wang, H. Chen, J. Law, H. Pu, S. Xie, F. Duan, Y. Sun, N. Liu, J. Yu, *Nat. Commun.* **2024**, 15, 644; c)Y. Zhou, X. Zhao, J. Xu, G. Chen, T. Tat, J. Li, J. Chen, *Sci. Adv.* **2024**, 10, eadj8567; d)R. H. Soon, Z. Yin, M. A. Dogan, N. O. Dogan, M. E. Tiryaki, A. C. Karacakol, A. Aydin, P. Esmaeili-Dokht, M. Sitti, *Nat. Commun.* **2023**, 14, 3320.

[6] a)S. Xu, C. M. M. Nunez, M. Souri, R. J. J. Wood, *Sci. Robot.* **2023**, 8, eadd4649; b)D. Wang, B. Zhao, X. Li, L. Dong, M. Zhang, J. Zou, G. Gu, *Nat. Commun.* **2023**, 14, 5067; c)W. Feng, L. Sun, Z. Jin, L. Chen, Y. Liu, H. Xu, C. Wang, *Nat. Commun.* **2024**, 15, 4222.

[7] a)X. Du, P.-P. He, C. Wang, X. Wang, Y. Mu, W. Guo, *Adv. Mater.* **2023**, 35, 2206302; b)D. Jiao, Q. L. Zhu, C. Y. Li, Q. Zheng, Z. L. Wu, *Accounts of Chemical Research* **2022**, 55, 1533; c)L. Tang, L. Wang, X. Yang, Y. Feng, Y. Li, W. Feng, *Progress in Materials Science* **2021**, 115, 100702; d)Z. L. Wu, M. Moshe, J. Greener, H. Therien-Aubin, Z. Nie, E. Sharon, E. Kumacheva, *Nat. Commun.* **2013**, 4, 1586.

[8] a)Z. Yang, Y. Wang, L. Lan, Y. Wang, X. Zhang, *Small* **2024**, n/a, 2401580; b)C. Li, X. Yang, Y. Wang, J. Liu, X. Zhang, *Adv. Funct. Mater.* **2024**, n/a, 2410659; c)C. Chen, H. Yu, T. Lai, J. Guo, M. Qin, Z. Qu, Y. Feng, W. Feng, *SusMat* **2023**, 3, 843; d)Y. Wang, Q. Guo, G. Su, J. Cao, J. Liu, X. Zhang, *Adv. Funct. Mater.* **2019**, 29, 1906198.

[9] a)M. Pontin, D. D. Damian, *Sci. Robot.*, 9, eadk9978; b)X. Guo, W. Tang, K. Qin, Y. Zhong, H. Xu, Y. Qu, Z. Li, Q. Sheng, Y. Gao, H. Yang, J. Zou, *Sci. Adv.*, 10, eadn6642.

[10] a)N. D. Naclerio, A. Karsai, M. Murray-Cooper, Y. Ozkan-Aydin, E. Aydin, D. I. Goldman, E. W. Hawkes, *Sci. Robot.* **2021**, 6, eabe2922; b)R. Dreyfus, Q. Boehler, S. Lyttle, P. Gruber, J. Lussi, C. Chautems, S. Gervasoni, J. Berberat, D. Seibold, N. Ochsenbein-Kölble, M. Reinehr, M. Weisskopf, L. Remonda, B. J. Nelson, *Sci. Robot.*, 9, eadh0298.

[11] a)C. Zhang, P. Zhu, Y. Lin, Z. Jiao, J. Zou, *Adv. Intell. Syst.* **2020**, 2, 1900166; b)Y. Jung, K. Kwon, J. Lee, S. H. Ko, *Nat. Commun.* **2024**, 15, 3510.

[12] D. R. Yao, I. Kim, S. Yin, W. Gao, *Adv. Mater.* **2024**.

[13] a)D. Yang, M. Feng, G. Gu, *Adv. Mater.* **2024**, 36; b)Q. Hu, E. Dong, D. Sun, *IEEE Trans. Robot.* **2023**, 39, 399.

[14] a)E. Del Dottore, A. Mondini, N. Rowe, B. Mazzolai, *Sci. Robot.*, 9, eadi5908; b)E. W. Hawkes, L. H. Blumenschein, J. D. Greer, A. M. Okamura, *Sci. Robot.* **2017**, 2, eaan3028; c)B. K. Johnson, M. Naris, V. Sundaram, A. Volchko, K. Ly, S. K. Mitchell, E. Acome, N. Kellaris, C. Keplinger, N. Correll, J. S. Humbert, M. E. Rentschler, *Nat. Commun.* **2023**, 14, 4516.

This article is protected by copyright. All rights reserved.

Author Manuscript

[15] a)E. H. Rumley, D. Preninger, A. S. Shomron, P. Rothemund, F. Hartmann, M. Baumgartner, N. Kellaris, A. Stojanovic, Z. Yoder, B. Karrer, C. Keplinger, M. Kaltenbrunner, *Sci. Adv.* **2023**, 9, eadf5551; b)J. Sun, E. Lerner, B. Tighe, C. Middlemist, J. Zhao, *Nat. Commun.* **2023**, 14, 6023.

[16] a)R. Baines, S. K. Patiballa, B. Gorissen, K. Bertoldi, R. Kramer-Bottiglio, *Adv. Mater.* **2023**, 35; b)Q. Ze, S. Wu, J. Nishikawa, J. Dai, Y. Sun, S. Leanza, C. Zemelka, L. S. Novelino, G. H. Paulino, R. R. Zhao, *Sci. Adv.*, 8, eabm7834.

[17] a)Y. Lin, G. Yang, Y. Liang, C. Zhang, W. Wang, D. Qian, H. Yang, J. Zou, *Adv. Funct. Mater.* **2020**, 30, 2000349; b)Z. Jiao, C. Zhang, J. Ruan, W. Tang, Y. Lin, P. Zhu, J. Wang, W. Wang, H. Yang, J. Zou, *Cell Reports Physical Science* **2021**, 2; c)S. Y. Kim, R. Baines, J. Booth, N. Vasios, K. Bertoldi, R. Kramer-Bottiglio, *Nat. Commun.* **2019**, 10, 3464.

[18] C. Zhang, Z. Zhang, Y. Peng, Y. Zhang, S. An, Y. Wang, Z. Zhai, Y. Xu, H. Jiang, *Nat. Commun.* **2023**, 14, 4329.

[19] a)K. Kobayashi, S. H. Oh, C. Yoon, D. H. Gracias, *Macromolecular Rapid Communications* **2018**, 39, 1700692; b)C. Yao, Z. Liu, C. Yang, W. Wang, X.-J. Ju, R. Xie, L.-Y. Chu, *Adv. Funct. Mater.* **2015**, 25, 2980.

[20] a)Y. Zhang, C. Wang, M. Yin, H. Liang, Q. Gao, S. Hu, W. Guo, *Angewandte Chemie International Edition* **2024**, 63, e202311678; b)Y. Zhao, C. Xuan, X. Qian, Y. Alsaid, M. Hua, L. Jin, X. He, *Sci. Robot.* **2019**, 4, eaax7112.

[21] a)A. Cangialosi, C. Yoon, J. Liu, Q. Huang, J. Guo, T. D. Nguyen, D. H. Gracias, R. Schulman, *Science* **2017**, 357, 1126; b)Z. Zhao, C. Wang, H. Yan, Y. Liu, *Adv. Funct. Mater.* **2019**, 29, 1905911.

[22] M. A. Robertson, J. Paik, *Sci. Robot.* **2017**, 2, eaan6357.

[23] M. G. B. Atia, A. Mohammad, A. Gameros, D. Axinte, I. Wright, *Adv. Sci.* **2022**, 9, 2203217.

[24] Q. He, R. Yin, Y. Hua, W. Jiao, C. Mo, H. Shu, J. R. Raney, *Sci. Adv.*, 9, eade9247.

[25] a)E. Del Dottore, A. Mondini, N. Rowe, B. Mazzolai, *Sci. Robot.* **2024**, 9, eadi5908; b)M. E. Tiryaki, Y. G. Elmacioglu, M. Sitti, *Sci. Adv.* **2023**, 9, eadg6438; c)Z. Xie, F. Yuan, J. Liu, L. Tian, B. Chen, Z. Fu, S. Mao, T. Jin, Y. Wang, X. He, G. Wang, Y. Mo, X. Ding, Y. Zhang, C. Laschi, L. Wen, *Sci. Robot.* **2023**, 8, eadh7852.

[26] a)D. Wang, C. Jiang, G. Gu, *IEEE Trans. Robot.* **2024**, 40, 606; b)S. Rahman, L. Wu, A. El Elmi, D. Pasini, *Adv. Funct. Mater.* **2023**, 33.

[27] a)T. F. Hansen, *Biosystems* **2003**, 69, 83; b)G. P. Wagner, M. Pavlicev, J. M. Cheverud, *Nature Reviews Genetics* **2007**, 8, 921.

This article is protected by copyright. All rights reserved.

Author Manuscript

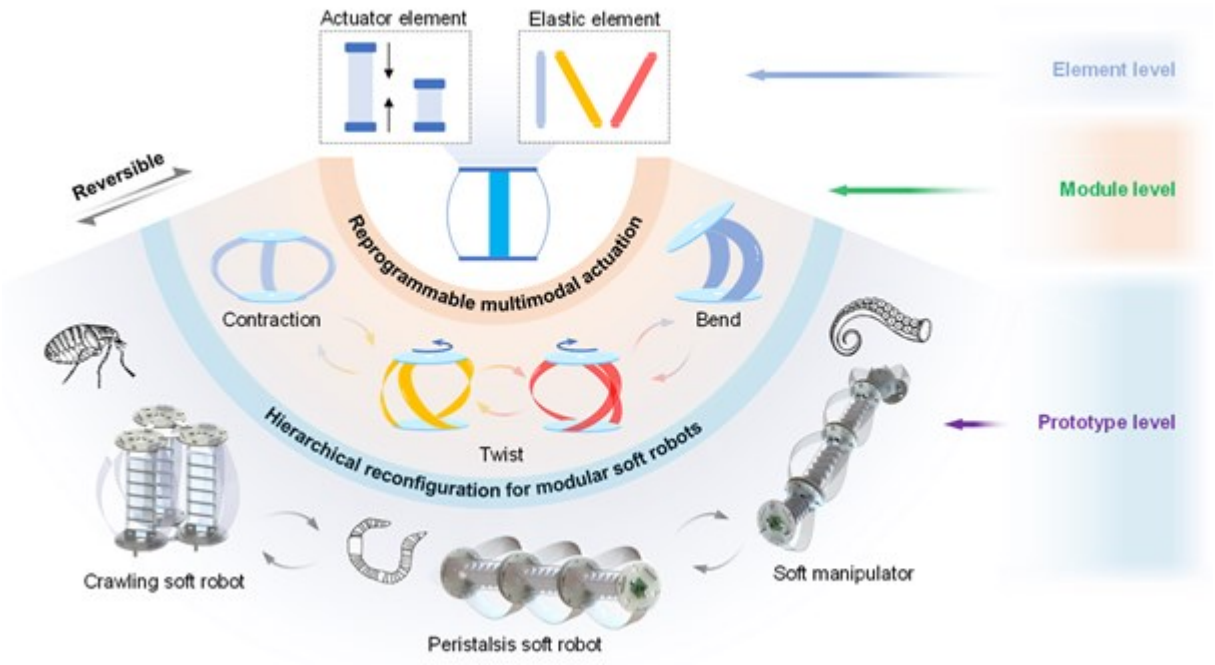


Figure 1. Conceptual design of the hierarchical reconfiguration with the levels of reprogrammable multimodal actuation induced by elastic beams, and reconfigurable soft robots assembled by basic modules of different actuating modes.

This article is protected by copyright. All rights reserved.

Author Manuscript

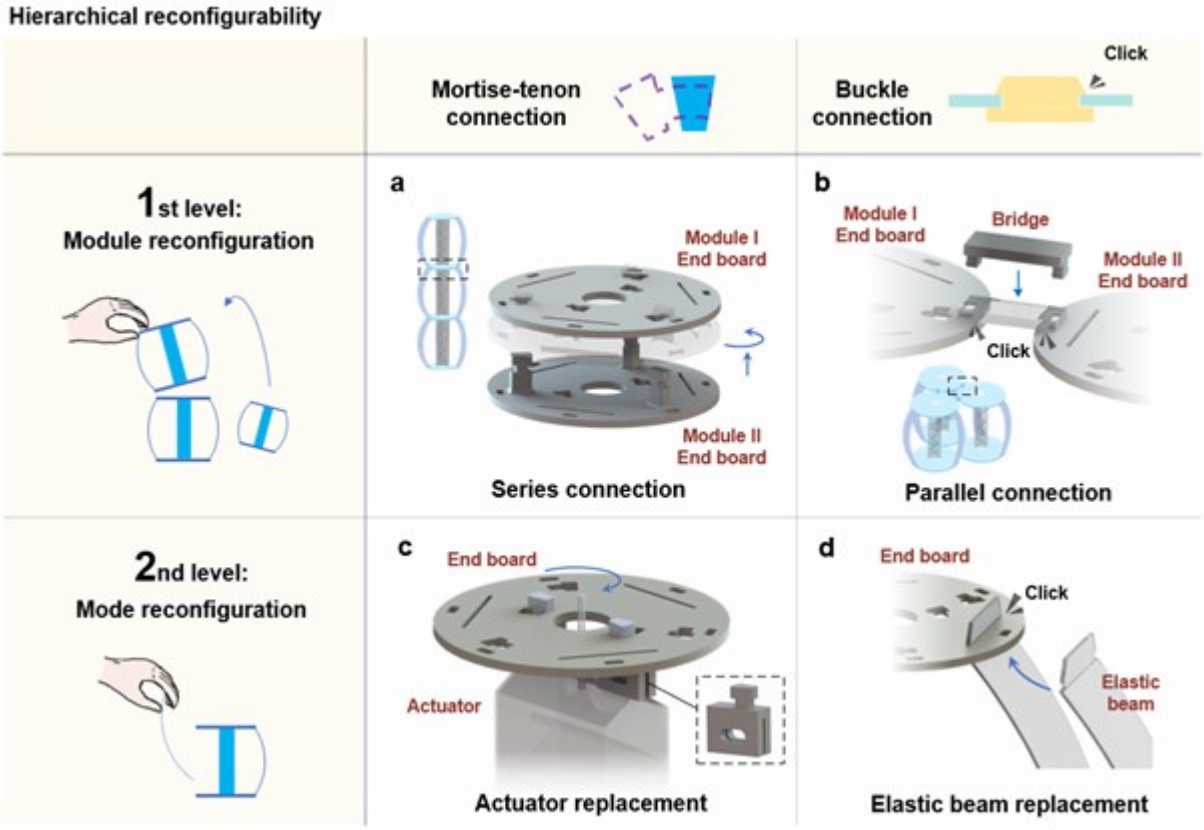


Figure 2. Depiction of the quick connecting methods to achieve hierarchical reconfigurability. (a) Series connection between modules achieved by the mortise-tenon structures on the end boards. (b) Parallel connection between modules with a bridge which contains buckle structures inserting into the corresponding holes on the end boards. (c) Actuator replacement achieved by mortise-tenon structure with connectors plugged to the end board and glued to the actuator. (d) Elastic beam replacement achieved by buckle structures on the ends of the beams.

This article is protected by copyright. All rights reserved.

Author Manuscript

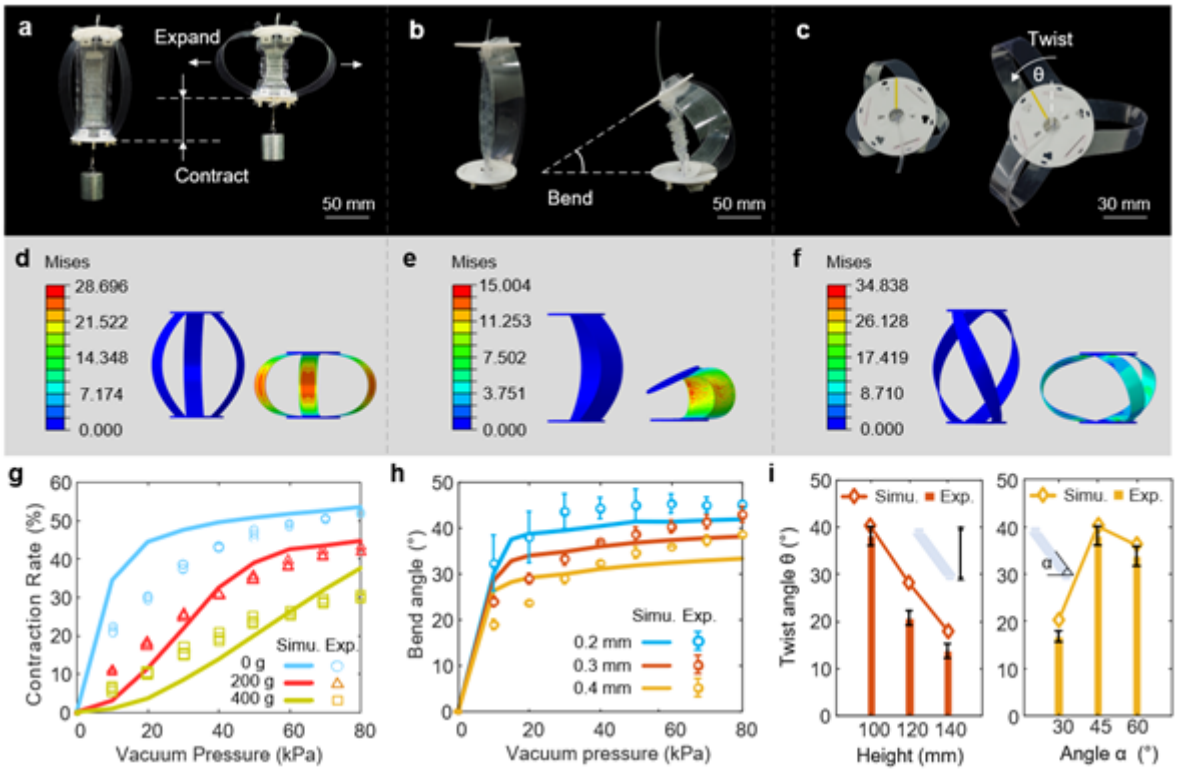


Figure 3. Performance of the multimodal modules. (a) Front view of the contraction module with a hanging load, showing a expand motion at the same time. (b) Front view of the bend module, in which the bend degree is defined by the angle between the end boards. (c) Vertical view of the twist module, assigning the rotation angle θ of the end board as the twist angle. (d), (e) and (f) Simulation of the loaded contraction module, bend module and twist module. (g) Measured contraction rate of the contraction module with load of 0 g, 200 g and 400 g, considering different actuating vacuum pressure. (Beam: size of 20×135 mm and thickness of 0.3 mm) (h) Measured bend angle of the bend module with beam thickness of 0.2 mm, 0.3 mm and 0.4 mm, considering different actuating vacuum pressure. (Beam: size of 20×135 mm) (i) Measured twist angle of the twist module considering different height of 100 mm, 120 mm and 140 mm (Beam: leaned angle of 45 ° and thickness of 0.3 mm, vacuum pressure: -80 kPa), and different leaned angle of 30 ° , 45 ° and 60 ° (Beam: height of 100 mm and thickness of 0.3 mm, vacuum pressure: -80kPa).

This article is protected by copyright. All rights reserved.

Author Manuscript

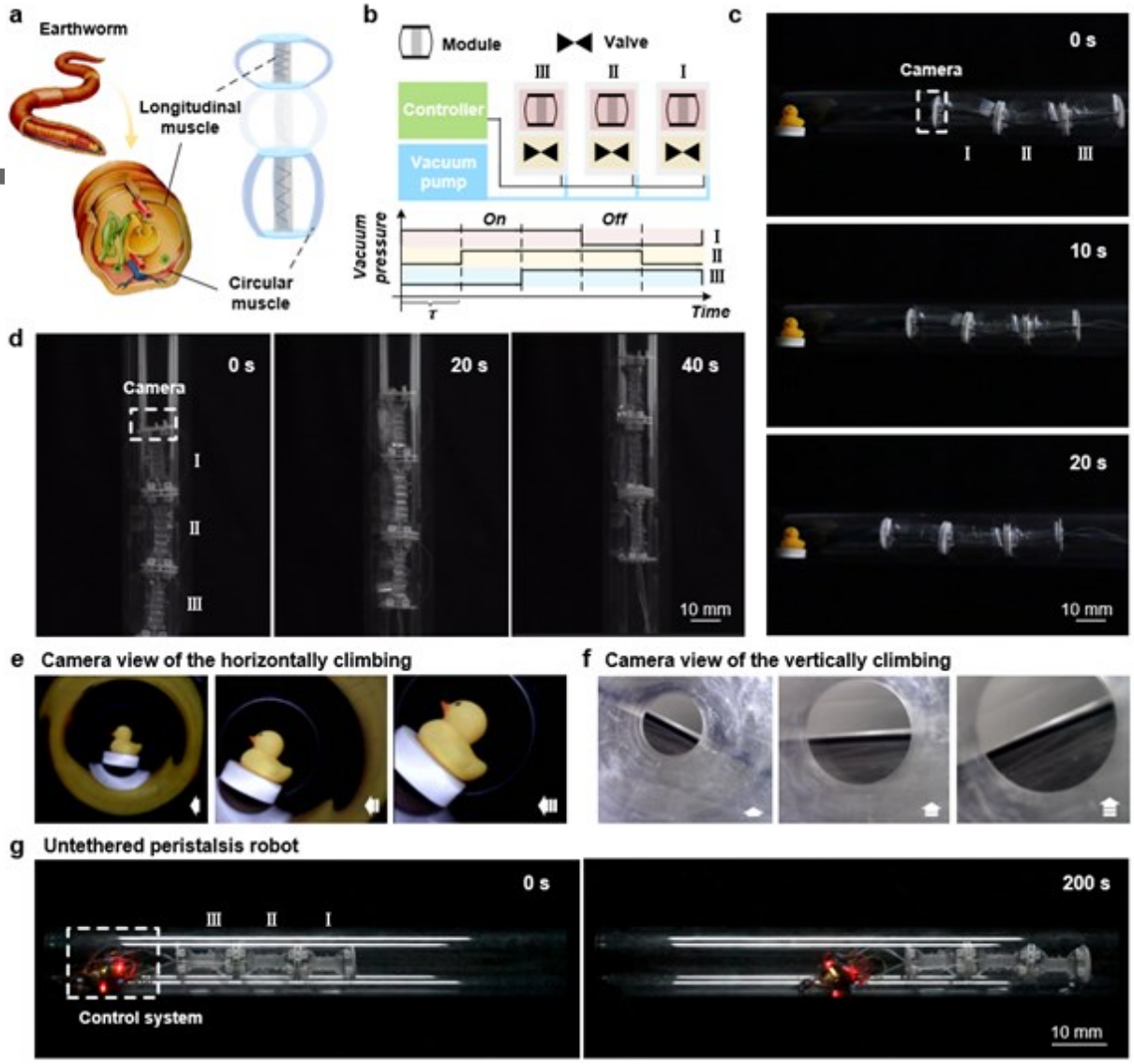


Figure 4. Peristalsis soft robot consisting of series connected modules. (a) Longitudinal muscle and circular muscle of earthworms and corresponding structures of the contraction module. (b) Distributed controlling system of the peristalsis soft robot and the instruction sequence to the vacuum pressure as the robot crawling forward, with each step time as τ. (c) Images of the peristalsis soft robot equipped with camera moving in the horizontal tube with speed of 6.7 mm/s. (d) Images of the peristalsis soft robot equipped with camera moving in the vertical tube with speed of 3.1 mm/s. (e) Camera view of horizontally climbing robot. (f) Camera view of the vertically climbing robot. (g) Images of the untethered peristalsis robot, with speed of 1.4 mm/s.

This article is protected by copyright. All rights reserved.

Author Manuscript

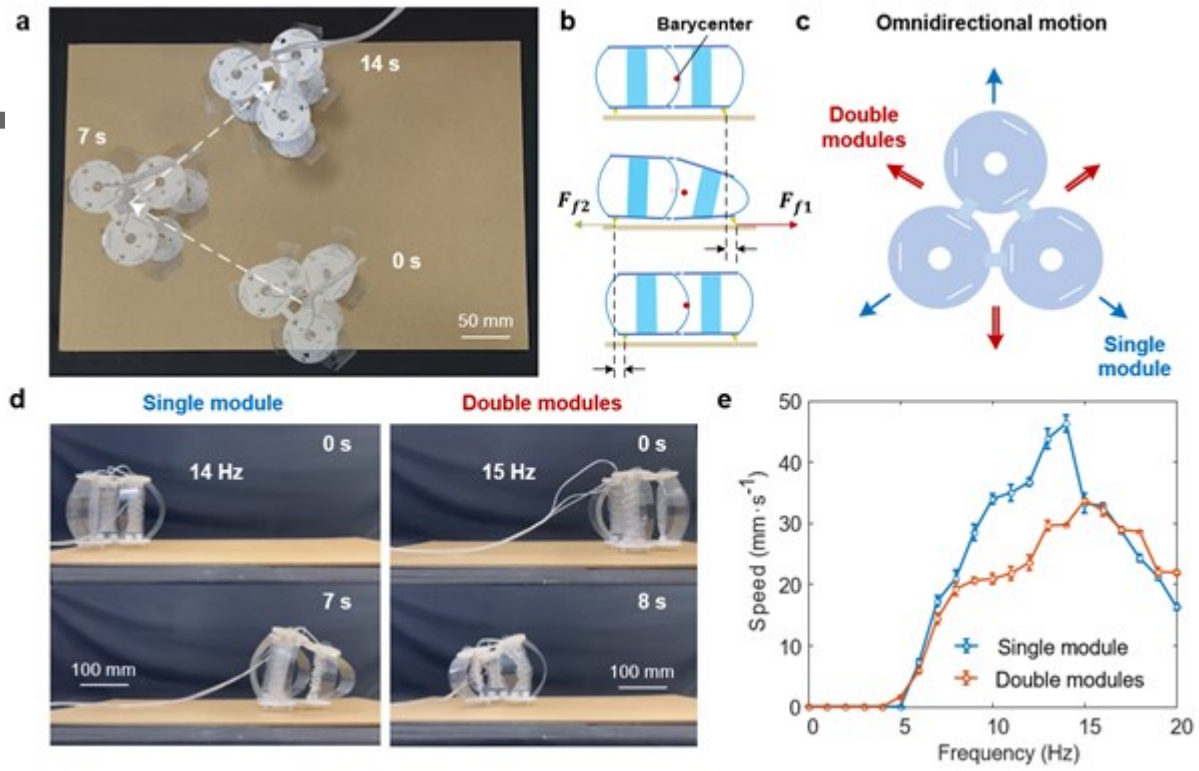


Figure 5. Crawling soft robot consisting of parallel connected modules. (a) Exhibition of a 3-module crawling soft robot able to moving and turning on the plane. (b) The moving progress of the crawling soft robot related to the barycenter's displacement. (c) Omnidirectional motion of the crawling soft robot enabled by single module actuating or double modules actuating. (d) Images of the crawling soft robot actuated with a single module leading the largest speed of 47 mm/s with actuating frequency of 14 Hz, and with double modules leading the largest speed of 34 mm/s with actuating frequency of 15 Hz. (e) Moving speed of the crawling soft robot on the horizontal plane with a single module actuated or double modules actuated, considering the actuating frequency from 0 Hz to 20 Hz.

This article is protected by copyright. All rights reserved.

Author Manuscript

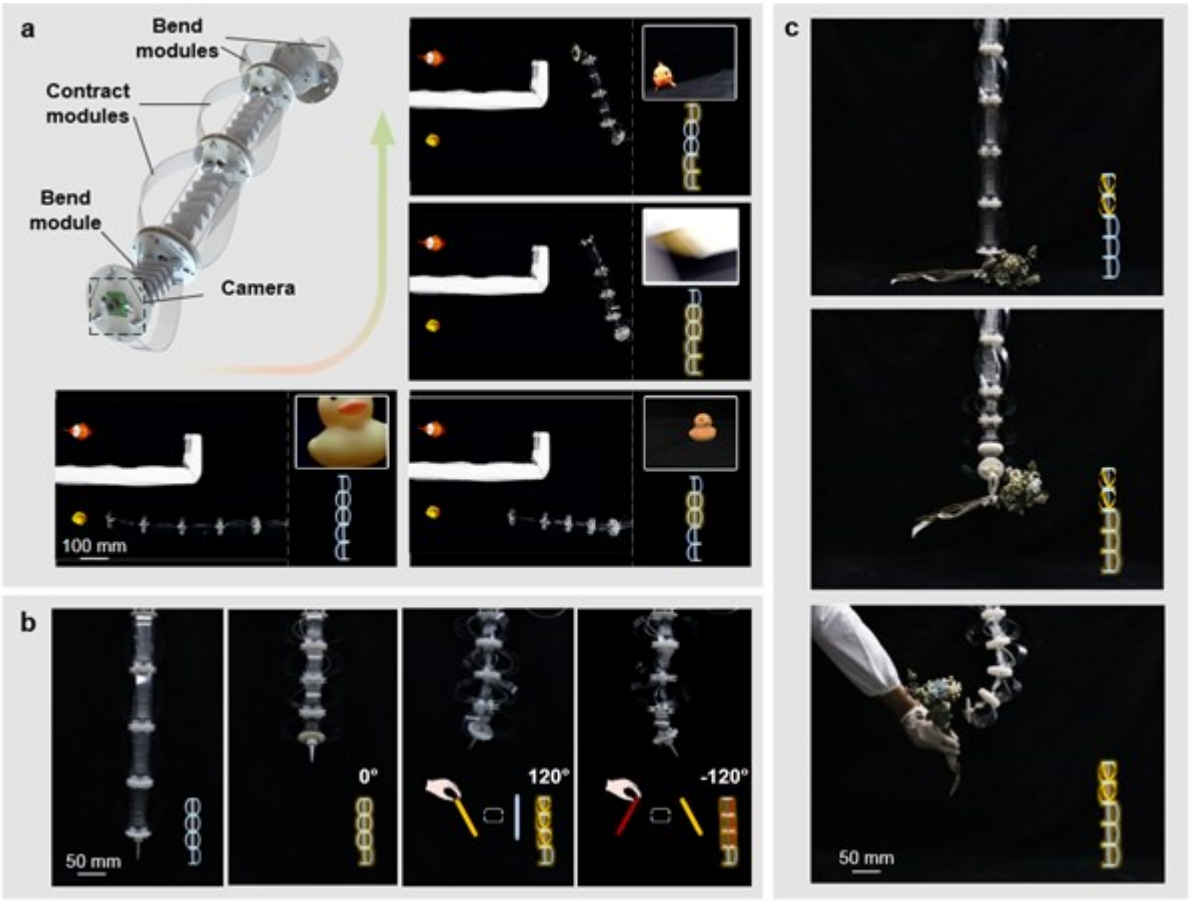


Figure 6. Soft manipulators consisting of multimodal modules. (a) A soft manipulator equipped with a camera on the end, able to explore the environment with controlled vacuum pressure and sequential instruction. (b) The reprogrammability of the soft manipulator, allowing the twist angle range from -120 ° to 120 ° with the replacement of the beams on the top three modules. (c) A manipulator consisting of two twist modules and three bend modules, accomplishing a human interaction task, i.e., catching and delivering a bunch of flowers.

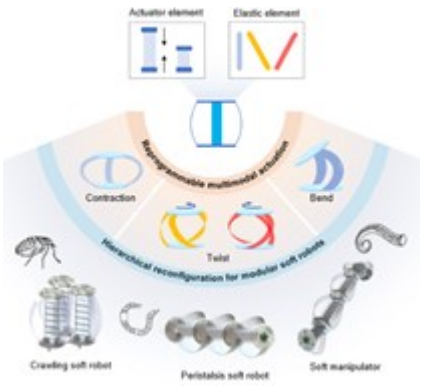
This article is protected by copyright. All rights reserved.

Author Manuscript

A new concept of hierarchically reconfigurable strategy and elastically-guided multimodal actuation design principle for modular soft robots is reported in this work. With the delicate experiments and analysis, the performances of the modules ~~is~~ are revealed. Subsequently, multi types of robots are demonstrated, including a tube detecting robot, a planar omnidirectional crawling robot and several soft manipulators.

Fuyi Fang, Wenbo Li*, Xinyu Guo, Huyue Chen, Guang Meng, Wenming Zhang*

Hierarchically Reconfigurable Soft Robots with Reprogrammable Multimodal Actuation



This article is protected by copyright. All rights reserved.